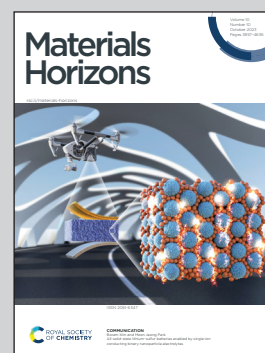


Showcasing research from Professor Inkyu Park's laboratory formerly at the Korea Advanced Institute of Science and Technology (KAIST), Daejeon, Republic of Korea.

A wearable colorimetric sweat pH sensor-based smart textile for health state diagnosis

The electrospun curcumin composite fiber-based colorimetric sweat pH sensor provides a rapid diagnosis of disease states such as cystic fibrosis. This work furnishes a convenient diagnosable clothing system.

As featured in:



See Jun-Ho Jeong, Inkyu Park *et al.*, *Mater. Horiz.*, 2023, 10, 4163.

Cite this: *Mater. Horiz.*, 2023,  
10, 4163Received 6th March 2023,  
Accepted 12th June 2023

DOI: 10.1039/d3mh00340j

rsc.li/materials-horizons

## A wearable colorimetric sweat pH sensor-based smart textile for health state diagnosis†

Ji-Hwan Ha,<sup>a</sup> Yongrok Jeong,<sup>ab</sup> Junseong Ahn,<sup>ab</sup> Soonhyong Hwang,<sup>b</sup> Sohee Jeon,<sup>b</sup> Dahong Kim,<sup>c</sup> Jiwoo Ko,<sup>ab</sup> Byeongmin Kang,<sup>ab</sup> Young Jung,<sup>a</sup> Jungrak Choi,<sup>a</sup> Hyeonseok Han,<sup>a</sup> Jimin Gu,<sup>a</sup> Seokjoo Cho,<sup>a</sup> Hyunjin Kim,<sup>a</sup> Moonjeong Bok,<sup>b</sup> Su A. Park,<sup>bd</sup> Jun-Ho Jeong<sup>ib</sup>\*<sup>b</sup> and Inkyu Park<sup>id</sup>\*<sup>a</sup>

Sweat pH is an important indicator for diagnosing disease states, such as cystic fibrosis. However, conventional pH sensors are composed of large brittle mechanical parts and need additional instruments to read signals. These pH sensors have limitations for practical wearable applications. In this study, we propose wearable colorimetric sweat pH sensors based on curcumin and thermoplastic-polyurethane (C-TPU) electrospun-fibers to diagnose disease states by sweat pH monitoring. This sensor aids in pH monitoring by changing color in response to chemical structure variation from enol to di-keto form via H-atom separation. Its chemical structure variation changes the visible color due to light absorbance and reflectance changes. Furthermore, it can rapidly and sensitively detect sweat pH due to its superior permeability and wettability. By O<sub>2</sub> plasma activation and thermal pressing, this colorimetric pH sensor can be easily attached to various fabric substrates such as swaddling and patient clothing via surface modification and mechanical interlocking of C-TPU. Furthermore, the diagnosable clothing is durable and reusable enough to neutral washing conditions due to the reversible pH colorimetric sensing performance by restoring the enol form of curcumin. This study contributes to the development of smart diagnostic clothing for cystic fibrosis patients who require continuous sweat pH monitoring.

### Introduction

Sweat contains useful information regarding human health conditions and can be used to diagnose serious illnesses, such as cystic fibrosis (CF),<sup>1,2</sup> dehydration,<sup>3</sup> and diabetes.<sup>4</sup> Above all,

<sup>a</sup> Department of Mechanical Engineering Korea Advanced Institute of Science and Technology, Daejeon 34141, Republic of Korea. E-mail: inkyu@kaist.ac.kr

<sup>b</sup> Department of Nano-manufacturing Technology Korea Institute of Machinery and Materials, Daejeon 34103, Republic of Korea. E-mail: jhjeong@kimm.re.kr

<sup>c</sup> Department of Applied Bioengineering, Graduate School of Convergence Science and Technology, Seoul National University, Seoul 08826, Republic of Korea

<sup>d</sup> Nano-Convergence Mechanical Systems Research Division, Korea Institute of Machinery and Materials, Daejeon 34103, Republic of Korea

† Electronic supplementary information (ESI) available. See DOI: <https://doi.org/10.1039/d3mh00340j>

### New concepts

Our study introduces a new wearable colorimetric pH sensor that can monitor cystic fibrosis patients' health status. We developed a curcumin-containing sensor that can detect changes in sweat pH, which can increase to pH 9 during disease exacerbation. The color of the curcumin-thermoplastic polyurethane (C-TPU) fibers changes from yellow to red when sweat pH increases, due to changes in light absorbance and reflectance caused by changes in the keto-enol structure. To create garments with the sensor, we used the thermal properties of TPU polymers and surface modification processes to ensure adhesion to different fabrics, including cotton, silk, spandex, and paper. This adhesive-free attachment enables the diagnosis of cystic fibrosis patients in their daily lives. We tested the practical application by attaching C-TPU to clothes for diagnosing cystic fibrosis in infants, children, and the elderly. The washable clothing attached with C-TPU can be easily cleaned using a neutral detergent, allowing for continuous diagnosis without affecting the sensor's performance.

the sweat pH is an important factor in diagnosing health conditions. For example, sweat pH can function as an essential signature for the deterioration of CF, which is one of the most common fatal genetic diseases affecting ~30 000 people in the United States and more than ~70 000 people worldwide.<sup>5</sup> CF patients are expected to live to 47 years old when continuous management is carried out in modern times.<sup>6,7</sup> The viscosity of blood flowing through the pulmonary blood vessels and airways increases with the progression of CF.<sup>5-7</sup> As a result of the increased mucus in their blood vessels and airways, patients have difficulty in controlling salt and moisture in their bodies. By clogging the blood vessels in the lungs with mucus, it causes an increase in the sweat pH level (from pH 5.5 to pH 9) because of the change in hydrogen, sodium and chloride ion concentration of the body.<sup>8,9</sup> The obstruction of airways caused by mucus resulting from cystic fibrosis exacerbations disrupts metabolic processes, leading to alterations in the levels of sodium and chloride ions in the body. Consequently, the pH rises due to changes in the concentration of hydrogen ions in the patient's exhaled sweat. CF symptoms appear within a year

of birth and can be suspected in newborns with frequent diarrhea, fatty stools, and respiratory infections. If the appropriate timing of treatment for the disease is missed, disease progression can lead to breathing difficulties, worsening lung function, and death.<sup>7</sup> Unfortunately, as a preventive method does not exist yet, frequent monitoring of physiological changes is significant for the safety of patient.<sup>10</sup> Therefore, patients with CF need to visit the hospital regularly to check their health condition and disease severity.

For these reasons, the disease state of CF patients has to be monitored continuously to prevent derived diseases. Many researchers have developed sensitive pH sensors for CF diagnosis and health state monitoring.<sup>11–19</sup> Various materials such as ionic liquid,<sup>11,17</sup> metal (Au or Pt),<sup>16,19</sup> and carbon-based electrodes<sup>15,18</sup> have been employed for pH sensors. Because of their fluidity and poor mechanical characteristics, the liquid membranes of ionic liquid-based pH sensors may suffer from reduced quantities of liquid after repeated sensing cycles.<sup>20</sup> The metal-based pH sensors can detect delicate pH levels, but their brittle electrode and packaging has limitations such as low flexibility and bulky scale measurement equipment regarding wearable sensor applications. The carbon composite-based pH sensor can be made soft and flexible but not biocompatible because of carbon materials such as carbon nanotubes and graphene that can cause cancer.<sup>21</sup> Furthermore, in previous research, almost all pH sensors required additional measurement equipment, which makes them difficult to be applied in wearable and simple diagnosis systems for continuous disease state monitoring.<sup>15,17,18</sup> The above-mentioned pH sensors have the disadvantage that sweat must be collected separately for pH measurement. As an alternative, several sweat pH sensors that can be directly attachable to the skin, based on colorimetric principles, have been developed. However, this type of sensor can be inconvenient for the user due to the irritation felt by attachment of them, the non-permeability of the attachable pH sensor and skin rashes caused by low biocompatibility of the base materials detecting pH.<sup>22</sup> Thus, a wearable colorimetric sweat pH sensor, a non-direct skin attachment system, with high permeability and biocompatibility is needed.<sup>11,23</sup> Furthermore, the wettability of the sweat sensors was another essential point for the high sensitivity and rapid response of wearable sweat sensors. Only when all of the aforementioned characteristics are taken into consideration, and the requirements of a sweat sensor that is comfortable to wear and can diagnose CF promptly can be achieved.

Therefore, we investigated a natural material that responds rapidly to variations in sweat pH for a wearable and diagnosable sweat pH sensor. Curcumin is one of the natural pH sensing materials derived from curcuma.<sup>24</sup> Curcumin powder and curcumin-based composites such as curcumin hydrogel and curcumin composite electrospun fiber have been used as pH level indicators,<sup>25</sup> such as in the determination of liquid/air pH conditions<sup>25–27</sup> and food freshness monitoring,<sup>26,28</sup> due to the specific colorimetric pH sensing properties of curcumin. Curcumin is also biocompatible and safe, making it suitable for wearable and biomedical sensing applications. However, the

fabrication of composites containing curcumin has been rarely attempted, hence the diversity of the composites is limited. Furthermore, homogeneous curcumin dispersion is required to fabricate a curcumin-based composite; however, manufacturing a composite with homogeneous curcumin embedded is technically challenging. In addition, low solubility in water and aggregation characteristics of curcumin make it difficult to develop a uniformly dispersed composite material. A flexible and stretchable curcumin-based composite has not yet been created, and its use as a sweat pH sensor on clothing has not been suggested either. This is due to the reported curcumin-based composite's low flexibility, which is caused by a limitation in the mechanical properties of the base materials, and the low adhesion forces caused by low surface energy (hydrophobicity) of curcumin.<sup>29–31</sup> Although curcumin-based composites containing biocompatible base polymer such as polycaprolactone have been suggested, these composites show poor stretchability due to their base polymer. These polycaprolactone/curcumin-based pH sensors are not suited for wearable applications because their brittleness restricts human mobility. Furthermore, due to the poor interfacial adhesion of curcumin, attaching the curcumin-based composite pH sensor to a fabric with a rough surface is challenging. A novel composite and method for improved adhesion are required to overcome the aforementioned limitations.

The aforementioned limitations must be overcome for diagnostic wearable applications for patients. Reusable health status monitoring sensors in garments, especially for CF patients who need constant monitoring, can be practical due to simpler diagnosis. They are crucial because they can be prescribed as soon as a condition is beginning to worsen. This study introduces a new strategy for overcoming the limitations of reported sweat pH sensors. We developed a wearable colorimetric sweat pH sensor based on a fabric-attachable curcumin/TPU composite that does not need additional measuring devices or direct attachment to the skin for CF diagnosis. This colorimetric pH sensor fabricated by electrospinning was thermally pressed and mechanically interlocked onto various fabrics, including cotton, silk, polyester span, and paper. The fabrication process was optimized with respect to adhesion forces for stable attachment between the colorimetric sensor and fabric, wettability for rapid sensing performance, and colorimetric sensitivity for easy and accurate diagnosis. The C-TPU was attached to special clothes, such as a baby saddler and patient clothes. The clothes with a C-TPU pH sensor were evaluated for pH sensing performance and reusability under neutral washing conditions.

## Results and discussion

Electrospinning (ESP) is one of the representative fabrication methods capable of producing micro- and nanoscale fiber-based fabrics with high porosity. ESP can be used to fabricate ultrafine fibers from various materials, including polymers, biomaterials, and inorganic materials.<sup>32,33</sup> Due to their superior permeability, the fabricated fiber-based fabrics are usually developed for wearable items such as clothes,<sup>34</sup> and masks.<sup>35</sup>

Fig. 1 illustrates the ESP-based research concept for real-time diagnosis of CF patients' health state by smart clothing. CF is a serious genetic disease that causes pulmonary vascular obstruction and mucus damage.<sup>5</sup> When the pulmonary vascular obstruction increases, the sweat pH increases to pH 9. In particular, the C-TPU pH sensor can be used to simply diagnose and monitor this disease state of patients with difficulty in movement, such as newborns or the elderly, by the color change properties of curcumin. The C-TPU attached to fabric (C-TPU/F) is fabricated through the optimized thermal pressing method. Furthermore, the sweat pH is measured by the color of the electrospun C-TPU pH sensor attached to specific clothes, such as baby swaddling and patient clothes.

The main challenging points in using this sensor are the stable attachment between the C-TPU and various fabric materials and the high sensitivity for accurate diagnosis. Firstly, the TPU's thermal forming properties (a gap between the glass transition;  $T_g$  and melting temperatures;  $T_m$ ) allow TPU-based composites to adhere to the fabric without using extra bonding materials. Therefore, in order to adhere the C-TPU pH sensor to the fabric, we adopted the thermal pressing approach. Applying high temperature and pressure cannot ensure adhesion while maintaining the C-TPU's fiber structure and porosity. Furthermore, the low adhesion between the fabric and C-TPU by the rough surfaces and difference of surface energy according to the materials causes delamination while in use. In particular, one aspect that hampers adherence is the hydrophobicity of curcumin due to its low surface energy. Therefore, the optimization of the surface binding force and fabrication process for attachment stability is required. Furthermore, the rough surface of the clothing fabric

caused by the weaving of the fibers makes adhering the C-TPU to the clothing difficult.

In Fig. 2(a), the fabrication process is illustrated. First, the C-TPU solution was prepared by stirring and sonicating the curcumin powder and TPU. The ESP was then performed for microscale functional fiber fabrication on the grounded metal plate. Here, the effect of plasma treatment on the surface binding forces in the fabrication process is investigated. We used  $O_2$  plasma treatment to improve and maintain the adhesion between the C-TPU sheet and various fabrics, forming hydroxyl groups on each surface. For strong bonding like covalent bonding and hydrogen bonding, a heat-pressing process was conducted. Furthermore, the TPU-based composite has a large gap between the glass transition temperature ( $58.6\text{ }^\circ\text{C}$ ) and melting temperature ( $148\text{ }^\circ\text{C}$ ), which helps the C-TPU to attach to fabrics by its thermal forming properties between the  $T_g$  and  $T_m$ . In Fig. S2 (ESI<sup>†</sup>), differential scanning calorimetry (DSC) and thermogravimetric analysis (TGA) results of TPU and C-TPU are shown. DSC analysis showed that the glass transition temperatures of the TPU and C-TPU fibers are  $58.6\text{ }^\circ\text{C}$  and  $55.4\text{ }^\circ\text{C}$ , respectively. The TGA results show that the thermal degradation of TPU and C-TPU occurs at  $280\text{ }^\circ\text{C}$  and  $306\text{ }^\circ\text{C}$ , respectively. At  $500\text{ }^\circ\text{C}$ , the TGA analysis reveals a weight loss of 91% for TPU and 75% for C-TPU. The following paragraphs introduce more detail about the deformation and thermoforming characteristics of C-TPU in different temperature conditions (between  $T_g$  and  $T_m$ , and  $>T_m$ ).

The temperature condition must be optimized for stable fiber structure and prevention of damage of curcumin and the C-TPU fiber shape by aggregation and thermal deformation. The morphological changes of C-TPU according to the process

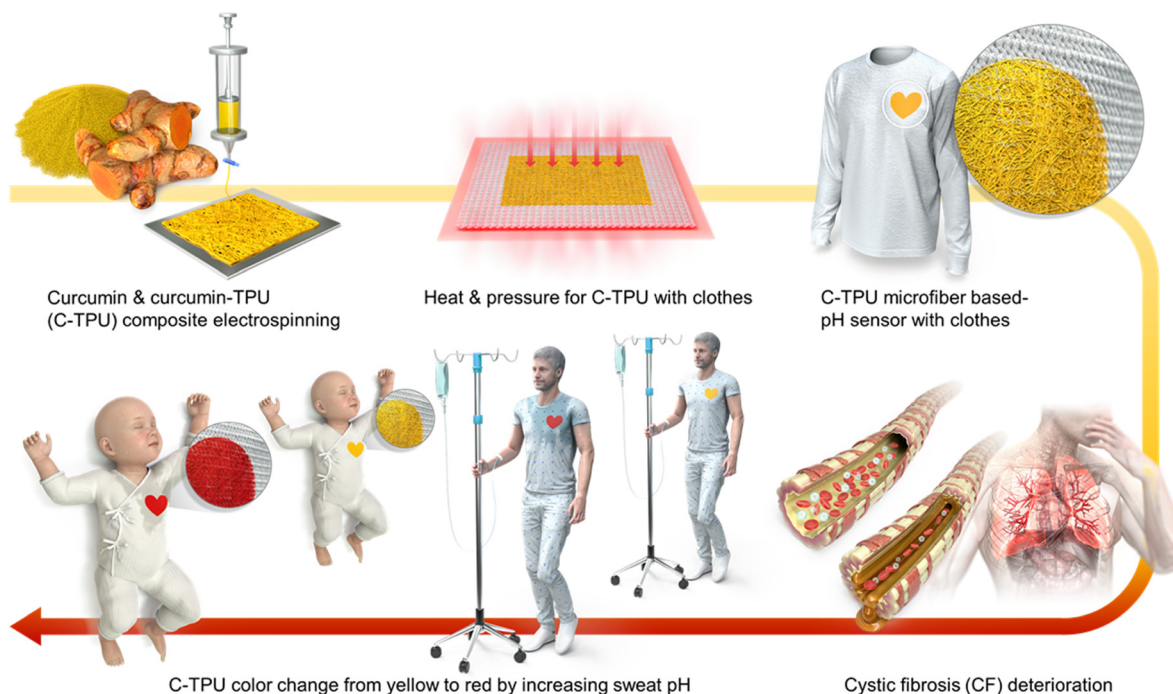
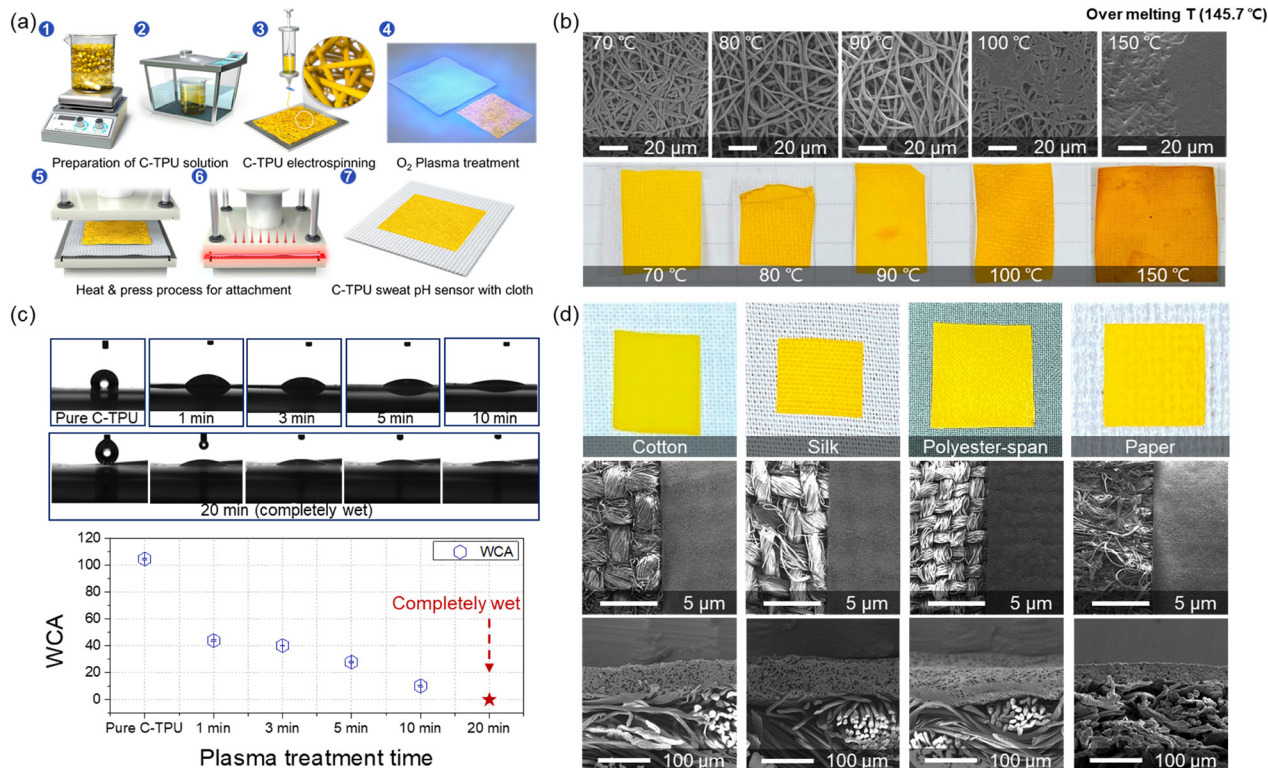


Fig. 1 Research overview. The scheme shows the electrospinning process of curcumin composite, attachment on fabric by heat and pressing, the C-TPU based colorimetric sensor attached to special clothing, sweat pH increase by CF deterioration, and simple and intuitive diagnosis of CF by sweat pH.



**Fig. 2** (a) Schematic of the fabrication process of the C-TPU based colorimetric sensor attached clothing. (1–3) C-TPU electrospinning. (4) O<sub>2</sub> plasma treatment to enhance the adhesion forces and to form the functional groups on the surface. (5 and 6) Attachment between various fabrics and the C-TPU patch by heat and pressure. (7) Completion of C-TPU/F. (b) Morphology variation of C-TPU fibers by an attachment process at different temperatures (70, 80, 90, 100, and 150 °C). (c) Water contact angle (WCA) for different O<sub>2</sub> plasma treatment times. As the O<sub>2</sub> plasma treatment time increases, the WCA decreases from 104.8° to 10.2°. After 20 min of O<sub>2</sub> plasma treatment, C-TPU was completely wetted by water owing to the enhanced hydrophilicity. (d) Photograph and SEM images (top and cross-section view) of C-TPU attached on cotton, silk, polyester, and paper fabrics.

temperature are shown in Fig. 2(b). The temperature condition is important for stable adhesion, structural stability, and function of C-TPU. TPU-based fiber sheets support the attachment to the substrate due to their thermal deformability that facilitates mechanical interlocking by reforming the shape of the substrate fabric's rough surface.

We attempted to optimize the process temperature conditions, focusing on the stable adhesion between the C-TPU and fabric without coagulation. The results demonstrated that the agglomeration of curcumin begins at temperatures higher than 90 °C. The yellow color of the C-TPU is partially changed to orange at some spots because of the agglomeration between the fibers. This phenomenon may worsen the colorimetric sensing performance of the diagnosable patches because of the non-uniform surface color. Furthermore, fibers are completely coagulated when the process temperature is over 100 °C. Therefore, a process temperature of 70 °C was used to achieve both stable sensor performance and prevention of fiber agglomeration.

In addition, the hydrophilicity of C-TPU was enhanced by O<sub>2</sub> plasma treatment. Fig. 2(c) shows the hydrophilicity of C-TPU with respect to the treatment time. The water contact angle (WCA) of the as-fabricated C-TPU was 104.8°. However, as the plasma treatment time increased, the WCA of C-TPU decreased. The WCAs for 1, 3, 5, and 10 min were 43.9°, 40.2°, 27.9°, and 10.2°, respectively. Furthermore, the C-TPU was completely

wetted by water after 20 min plasma treatment. The WCA was continuously maintained after 7 days (Fig. S1, ESI†). These results indicate that plasma treatment improves the adhesion of the interfaces by surface modification (e.g. hydroxyl group formation)<sup>36</sup> and helps the sweat absorption for efficient reaction on the diagnosable patch. Therefore, 20 min plasma treatment time was selected because of the superior wetting properties and adhesion force enhancement. Also, it should be noted that this long plasma treatment time did not cause visible damage to the fiber structure (Fig. S3, ESI†). Moreover, the photographs and SEM images of the fabricated C-TPU/F according to the kinds of fabric are presented in Fig. 2(d). The plasma-treated C-TPU has improved interfacial adhesion and can be attached to various fabrics, such as cotton, silk, polyester, and paper. The electrospun diagnostic patch of 80 μm thickness was stably adhered to cloth substrates with various woven structures.

We observed the basic properties of C-TPU fibers fabricated using ESP. The morphology of a C-TPU fiber is shown in Fig. 3(a). The SEM image reveals a stable fiber morphology without any beads. The diameter of the C-TPU fibers is distributed from 0.6 μm to 2.4 μm, with most of them between 1 μm and 2 μm (diameter mean: 1.5 μm, standard deviation: 0.4 μm). Fourier transform infrared spectroscopy (FTIR) analysis of the C-TPU sheet in Fig. 3(b) shows the OH group (3400–3200 cm<sup>-1</sup>) and NH group (3406 cm<sup>-1</sup>), which are the chemical

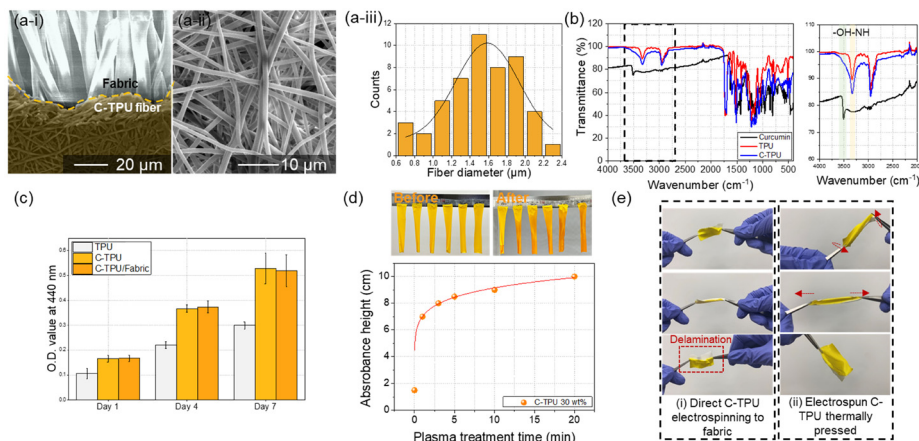


**Fig. 3** Characteristics of the electrospun C-TPU fibers. (a) The SEM images show the (i) C-TPU/F, and (ii) C-TPU fiber morphology. (iii) C-TPU fiber diameters are distributed from  $\mu\text{m}$  0.6 to 2.4  $\mu\text{m}$  (mean: 1.5  $\mu\text{m}$ , standard deviation: 0.4  $\mu\text{m}$ ). (b) FTIR analysis of curcumin, TPU, and C-TPU for compositional verification. (c) Cell proliferation properties of TPU, C-TPU, and C-TPU with fabric for seven days (WST-1). (d) Wettability of C-TPU according to  $\text{O}_2$  plasma treatment time (C-TPU height: 10 cm with: 2 cm). The wetted area of C-TPU is increased by increasing the treatment time. (e) Flexibility and stretchability of C-TPU. The electrospun C-TPU thermally pressed case (ii) having enhanced adhesion compared to direct C-TPU electrospinning to fabric (i) in stretching and twisting conditions.

structures within the curcumin and TPU, respectively. We also confirmed the biocompatibility of C-TPU through cell proliferation performance. In Fig. 3(c), the water-soluble tetrazolium salt (WST-1) assay results of the fibroblast cell proliferation for seven days are shown. The optical density value (OD value) at 440 nm is increased continuously from 0.1 to 0.3 (TPU) and approximately 0.5 (C-TPU) for seven days because of the increased cell proliferation, which verifies the biocompatibility of TPU and C-TPU. In particular, C-TPU shows superior cell proliferation performance because of antioxidant and therapeutic properties, scavenging oxygen free radicals, inhibiting lipid peroxidation, and cellular macromolecule protection (including DNA from oxidative damage) from curcumin.<sup>37</sup> Wettability enhancement results of C-TPU with a base buffer solution (pH 8) according to  $\text{O}_2$  plasma treatment time due to the surface modification (forming hydroxyl groups) is verified in Fig. 3(d). The 20 min plasma-treated C-TPU was completely wetted in 3 min while non-treated C-TPU got wetted only in the pH buffer solution contact area. When the treatment time increased, the wetting area was increased by higher surface energy and formation of hydroxyl groups on the surface. This means that the sweat absorbance performance of C-TPU can be enhanced by increasing the plasma treatment time. In Fig. 3(e), the flexibility and stretchability of C-TPU/F were characterized. The C-TPU directly electrospun into a fabric was delaminated from the fabric by twisting and stretching because of the low adhesion force between them. In contrast, thermally pressed C-TPU/F was stably attached to the fabric without delamination owing to the superior adhesion by thermal pressing and  $\text{O}_2$  plasma treatment. Further, the C-TPU attached on various fabrics (silk, polyester span, and paper) showed superior adhesion by plasma treatment (Fig. S4, ESI<sup>†</sup>). In addition, Fig. S5 (ESI<sup>†</sup>) shows the mechanical properties of the three materials: 100% cotton fabric, C-TPU, and C-TPU/F (after  $\text{O}_2$  plasma treatment). Through a tensile test, we found that the fabric

has a maximum strain of 30% and a maximum stress of 32.5 MPa. Similarly, the C-TPU exhibited a maximum strain of 700% and a maximum stress of 22.5 MPa. Notably, in the case of C-TPU/F, the fabric was broken first with a maximum stress of 41.4 MPa and a maximum strain of 30%. Subsequently, the C-TPU material showed failure with a maximum stress of 17.8 MPa and a maximum strain of 640%.

To optimize the color change characteristics of the C-TPU pH colorimetric sensor for diagnosis of CF state by sweat, the color change in base conditions ( $> \text{pH}$  7) of the curcumin content was observed. As shown in Fig. 4(a), the color of C-TPU/F (cotton) rapidly changes from yellow to red in 3 min because of the chemical structure change by enol-keto tautomerization. Therefore, under basic conditions, this colorimetric sweat pH sensor color was changed by the H-atom transfer of curcumin at an increased pH ( $> 7$ ). Curcumin exists in a neutral form (H3A), H2A<sup>-</sup>, HA2<sup>-</sup>, and A3<sup>-</sup> at pH 1–7, pH 7–8, pH 8.5, and pH  $> 9$ , respectively (Fig. S6, ESI<sup>†</sup>).<sup>38,39</sup> The chemical structure of curcumin affects the absorption and reflection of light, allowing pH to be distinguished by color. Consequently, utilizing the color change of C-TPU/F, pH may be distinguished from the naked eye. This colorimetric sensor is appropriate for sweat based health monitoring applications owing to its rapid reaction. Moreover, the level of curcumin present plays a significant role in the observable alteration of color. The pH sensor made of C-TPU with a curcumin content of 30 wt% displayed a more pronounced color change compared to C-TPU variants with lower curcumin contents (5, 10, and 20 wt%). Additionally, by combining curcumin with natural acid-reactive pH indicators like anthocyanins, it is anticipated that the color change could be achieved across a broader pH range. The color change of C-TPU/F according to pH conditions is indicated on the CIE 1931 color space in Fig. 4(b). The C-TPU/F color difference was little (yellow and dark yellow) according to the curcumin concentration in the control condition (atmospheric condition;



**Fig. 4** The colorimetric pH sensing performance of C-TPU/F. (a) Color change of C-TPU/F by base conditions (pH 8 and 9) according to the curcumin contents (curcumin contents: 5, 10, 20, and 30 wt%) for 3 min. The left image shows the color change of C-TPU/F by pH buffer solutions. The picture on the right shows how the C-TPU/F color change is completed after an hour for comparison. (b) CIE 1931 color space according to pH conditions (normal atmospheric conditions (pH 6), pH 8 and 9). When the curcumin contents increased, the reddish color was clearer in the pH 8–9 conditions. (c) C-TPU/F color recovery test for repeated use of the colorimetric sensor with cotton fabric. The C-TPU/F color changed from yellow to red at pH 9. In addition, the C-TPU/F color recovered from red to yellow at pH 7. (d) FTIR analysis of C-TPU under various pH conditions (pH condition: pH 7–12). The peaks at  $1431\text{ cm}^{-1}$  and  $1360\text{ cm}^{-1}$  are the carboxyl group and phenol group, respectively.

pH 6). However, under basic conditions (pH 8 and 9), the high content C-TPU showed a marked color change to red with a significant difference from that of the low content C-TPU. This is because of the increase in the amount of curcumin, which responds to the pH change, within the C-TPU fiber. A distinct color change at pH 8–9 (orange-red color) is expected to allow for immediate diagnosis by sweat from CF patients.

The reusability of wearable devices is very important for long-term usage in daily life. C-TPU/F can be reused because the curcumin color change reaction is reversible according to the pH conditions (under pH 7: yellow, pH 8: orange, pH 9: red). In Fig. 4(c), cross-shaped C-TPU/F is changed to red at pH 9. After the reaction, the red C-TPU/F is changed back to yellow at pH 7. In neutral or acid conditions (*i.e.* healthy state) and a washing process with a neutral detergent, the C-TPU/F color is recovered because of the chemical structure recovery (H-atom binding) of curcumin to the enol form.

Furthermore, the durability of C-TPU fibers is verified in pH 8–9 conditions (Fig. S7, ESI<sup>†</sup>). However, when the pH exceeds 11, the C-TPU fibers are degraded due to the curcumin dissolution properties in base solution by solubility change. Additionally, we tried to verify the principle of curcumin color change by H-atom

movement in the base environment through FTIR analysis. Fig. 4(d) shows the variations of carboxyl and phenolic group peaks. When the pH increased from pH 7 to pH 12, the OH bending of the carboxyl and phenol groups decreased because of the H-atom separation of curcumin.

For the demonstration of wearable applications, a clover-shaped C-TPU pH sensor was attached to the baby's swaddling and patient clothing, as shown in Fig. 5(a) and (b). These clothing demonstrations show the possibility of easily diagnosing the disease states of CF patients. The clover-shaped C-TPU pH sensor attached to the swaddling clothing was wetted to the same extent as sweat through the clothing inside with buffer solutions of pH 8, 9, and 10, respectively.

When the pH buffer solution permeates into the clothing and is delivered to the colorimetric pH sensor, its color changes depending on the pH. The colorimetric sensor can be fabricated in various sizes by cutting the electrospun C-PTU. The sensors in various shapes can be attached to clothing (Fig. S8, ESI<sup>†</sup>). For comparison, color points of C-TPU/F according to the pH conditions appeared on the CIE 1931 color space, as shown in Fig. 5(c). As the pH increased sequentially from control (pH 7) to pH 10, the coordinates in the color space also tended to shift from yellow to red. The significant change in color space occurred at pH 8, and there was a color difference between pH 9 and 10, but it was not significant. Color-changed C-TPU pH sensors can be reused by washing them with a neutral detergent. We demonstrated the color recovery of C-TPU/F after color change by increasing the pH using a washing machine and detergent, as depicted in Fig. 5(d). After the washing process, the color of C-TPU/F returned to yellow. Furthermore, in Fig. S9 (ESI<sup>†</sup>), we observed the nominal color (under pH 7) and color change by pH (*i.e.* pH 7 to 9) of the C-TPU by repeated laundries. Throughout 10 cycles of laundry, the C-TPU material exhibits a minimal change in the nominal color in the CIE 1931 color space. Specifically, the difference is found to be less than 3.8% in the *x*-coordinate and 4.4% in the *y*-coordinate. Under pH 9, the color variation in the CIE 1931 color space is found to be up to 1.4% in the *x*-coordinate and 2.8% in the *y*-coordinate. In conclusion, the colorimetric sensing of C-TPU is found to be stable after repeated cycles of laundry with neutral detergent. Therefore, this reusable sensor-integrated garment is appropriate for patients requiring continuous observation of disease progression. Furthermore, it has the advantage of more intuitively diagnosing CF patients, even without expertise, or in a weak person, such as a baby or the elderly, when the illness development is difficult to predict.

## Experimental section

### Materials

Curcumin powder (Sigma Aldrich, USA) from *curcuma longa* (Turmeric) and TPU film (WOOJIN, Korea) of molecular weight  $M_w = 80\,000$  were used. Ethyl acetate (EA, DUKSAN, Korea) and *N,N*-dimethylformamide (DMF, DUKSAN, Korea) were used for the electrospinning solvent of curcumin and TPU. pH buffer

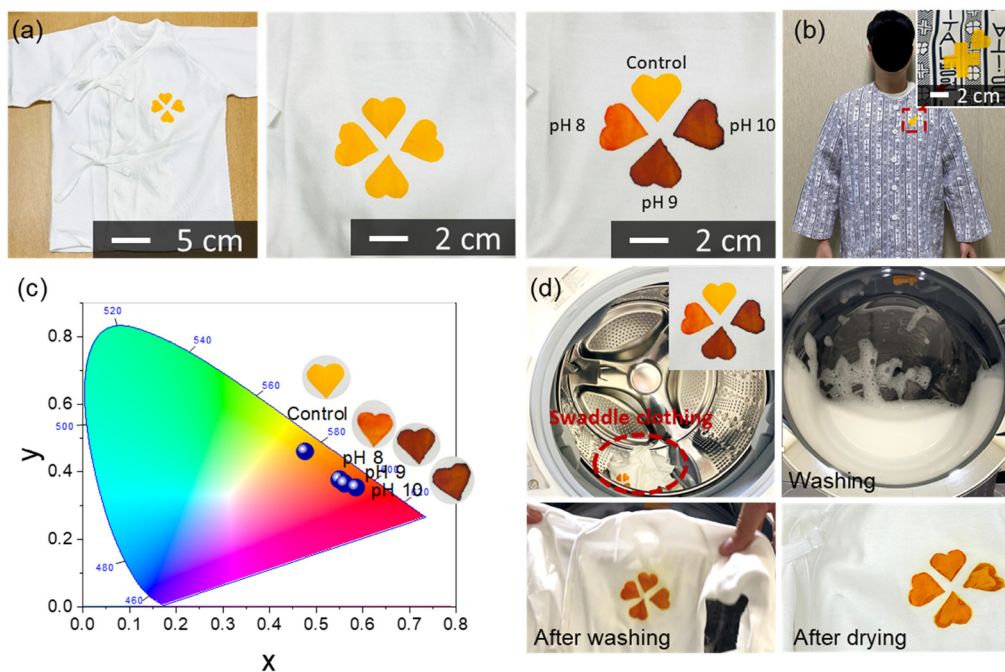


**Fig. 5** Clothing with a colorimetric sweat pH sensor (C-TPU). (a) Baby swaddling clothing with C-TPU pH sensors. The pH buffer solution changed the color of each cloverleaf shape C-TPU/F. (b) Patient clothing with a C-TPU (cross and heart shape) pH sensor. (c) CIE 1931 color space of each cloverleaf shape color on a baby swaddling cloth by pH condition. When the pH condition increased from pH 7 to pH 10, the C-TPU color changed from yellow to red. (d) The color of the C-TPU patch was recovered by washing the swaddle clothing in a washing machine with a neutral detergent.

solution (pH 7–11) was purchased from DUKSAN. The fabrics (cotton, silk, and polyester) were purchased from Zentex., Co., Ltd (Korea) The baby swaddling and patient clothing were purchased at the cloth market.

### Electrospun C-TPU fabric patch fabrication

For C-TPU microfiber fabrication, we conducted ESP. Before the ESP, the C-TPU solution was fabricated (Fig. 2(a)). First, curcumin and TPU were dissolved in EA and DMF (1 : 1 volume ratio). The curcumin content was 5, 10, 20, and 30 wt% compared to the TPU, and the TPU content was set to 15 wt% compared to the EA and DMF mixture solution. The C-TPU solution was stirred for 4 h at 50 °C using a magnetic stirrer (500 rpm). Next, the C-TPU solution was sonicated by a bath type of sonication machine (Branson, USA). After mixing the solution, the ESP was conducted for 2 h (condition: 1.5 mL h<sup>-1</sup> of nozzle speed, 20 kV of input power, 15 cm of height, 10 cm × 10 cm area) by the electrospinning machine (Nano NC, Korea). The C-TPU sheet was dried in a vacuum oven for one day.

The fabricated C-TPU can be cut into the desired shape. After the cutting of C-TPU, the O<sub>2</sub> plasma treatment of C-TPU and fabric (cotton, silk, polyester, and paper) was conducted for 20 min (20 min main fabrication condition, comparison condition: 0, 1, 3, 5, and 10 min) in 50 W of power and 50 sccm of O<sub>2</sub> flow rate by a plasma treatment machine (Femto science, Korea). The heat press process was conducted at various temperature conditions (60 °C: main fabrication condition, 80, 100, 120, and 150 °C) by 5 bar of pressure for 10 min.

C-TPU attached clothing was fabricated using the same method as the fabrication process.

### Characteristic

We observed the morphology of C-TPU and the fabric by SEM (Hitachi). The DSC analysis was conducted using a modulated differential scanning calorimeter (Netzsch) to 250 °C. The TGA analysis was conducted by a Max Res TGA (Mettler) to 800 °C. The diameter of the C-TPU fibers was measured by SEM image and Image J program. The WCA was measured by a water contact angle detection machine (KRÜSS Scientific, Germany). The 20 min treated C-TPU's WCA was measured for 7 days. FTIR analysis (range: 4000–400 cm<sup>-1</sup>) was conducted by FTIR spectrometer (Thermo Fisher Scientific Instrument, Korea). Various pH conditions C-TPU, curcumin, and TPU were observed by FTIR spectrometer. The wettability of C-TPU was observed through the pH 8 buffer solution included set up. The C-TPU height and width are 10 cm and 2 cm each. It was poured from only 1.5 cm height for 3 min (Fig. S10, ESI<sup>†</sup>).

### Cell culture

NIH3T3 cells, which is a fibroblast cell line isolated from a mouse, were used for cell assay of the TPU, C-TPU and C-TPU/fabric. The cells were cultured in Dulbecco's Modified Eagle's Medium (DMEM; Gibco, USA) supplemented with 10% fetal bovine serum (FBS) and 1% penicillin (Gibco, USA). TPU-based compositions were cultured at 37 °C with 5% CO<sub>2</sub> conditions. The medium was changed every 2 or 3 days.



### Cell proliferation assay

To investigate the cytotoxicity of TPU, C-TPU, and C-TPU/fabric, the WST-1 cell proliferation assay (Premix WST-1 Cell Proliferation Assay System; Takara, Japan) was used to measure mitochondrial dehydrogenase activity. They were sterilized with 70% ethanol for 1 min and washed using phosphate buffered saline (PBS; Hyclone, USA) 3 times to remove ethanol.  $5 \times 10^4$  cells per sterilized sample were seeded in a clean bench. They were cultured for 1, 3 and 7 days in an incubator. The reagent was prepared by mixing the WST-1 solution and DMEM media at a ratio of 10 : 1. Then, 500  $\mu\text{L}$  of the reagent was added in per sample and incubated for 1 hour. The reacted supernatant was extracted as 100  $\mu\text{L}$  in a 96 well plate and the absorbance was measured at 440 nm using a microplate reader (SpectraMas iD3; Molecular Devices, USA).

### pH colorimetric sensing test

pH colorimetric sensing performance of C-TPU was verified using the pH buffer solution (pH 7–11). The pH buffer solution was poured on the Petri dish, and C-TPU attached fabric was posed on the solution droplet (sweat). The observation of the C-TPU color was conducted by microscope. Furthermore, the color value was changed to the CIE 1931 color space value. In the color recovery test, we first used pH 9 buffer solution and pH 7 buffer solution to recover the yellow color. The pH colorimetric sensing performance of C-TPU attached clothing was observed through the above process using a pH buffer solution. Furthermore, this clothing was generally washed by a washing machine (LG Electronics, Korea).

## Conclusions

In this study, we developed a curcumin-based colorimetric sweat pH sensor for health monitoring. Using the thermal adhesion characteristics of C-TPU, attempts were made to combine it with fabrics of various materials and apply it to special clothes, such as baby swaddling and patient clothing. An optimized process for the application was developed, and the basic characteristics of the manufactured C-TPU/F and the biocompatibility for clothing applications were verified. In addition, the optimization of curcumin content for sensitive and intuitive color change and the width of the color change according to the content were observed. The chemical structure change was analyzed through FTIR, and the possibility of repeated use was verified by changing the chromaticity and restoring the color after washing using neutral detergent through an actual clothing demonstration. These colorimetric sweat sensors that are easily combined with such clothing are appropriate for diseases that require continuous observation and are expected to help in the fast monitoring of patients as the disease intensifies.

Through the findings of this study, it is expected that it will be possible to maintain the health of patients, such as children or the elderly, and to respond rapidly to the progression of diseases such as CF. This colorimetric pH sensor can be

attached to the fabric of shoes, tents, and sails as well as clothing, and can detect pH in various environments. At this stage, color changes by pH conditions are visually distinguished, but if real-time color detection performance using a photodetector is added in the future, sweat sensor clothing can be developed to enable faster and more accurate diagnosis by quantification of the pH condition.

## Author contributions

The manuscript was written based on contributions from all authors. J.-H. Ha conducted the experiments, analyzed the data, and wrote the manuscript. J.-H. Ha, Y. Joeng, J. Ahn, J. Ko, and S. Hwang discussed the results of the C-TPU based colorimetric sensor fabrication and bio-application. S. Jeon, M. Bok, and J.-H. Jeong discussed the results of  $\text{O}_2$  plasma treatment for adhesion improvement between C-TPU and various fabric. D. Kim and S. A. Park supported the cell proliferation experiments. B. Kang, Y. Jung, J. Gu, H. Han, and J. Choi discussed the results of the C-TPU composite analysis. S. Cho and H. Kim discussed the method of C-TPU attachment on specific clothing. J.-H. Jeong and I. Park contributed to the overall direction of the project. All authors have approved the final version of the manuscript.

## Conflicts of interest

There are no conflicts to declare.

## Acknowledgements

This work was supported by a National Research Foundation of Korea (NRF) grant funded by the Korean government (MSIT, No. 2021R1A2C3008742); Technological Development Program (S3130635) funded by the Ministry of SMEs and Startups (MSS, Korea); Basic Research Program of KIMM (Korea Institute of Machinery and Materials, NK242C); and the Development Program of Machinery and Equipment Industrial Technology (20018235, Development of inline nano-imprinter for nano photonic device) funded by the Ministry of Trade, Industry & Energy (MI, Korea).

## Notes and references

- 1 F. Ratjen, S. C. Bell, S. M. Rowe, C. H. Goss, A. L. Quittner and A. Bush, *Nat. Rev. Dis. Primers*, 2015, **1**, 15010–15028.
- 2 H. Brody, *Nature*, 2020, **583**, S1.
- 3 R. M. Morgan, M. J. Patterson and M. A. Nimmo, *Acta Physiol. Scand.*, 2004, **182**, 37–43.
- 4 D. Bruen, C. Delaney, L. Florea and D. Diamond, *Sensors*, 2017, **17**, 1866–1886.
- 5 T. S. Cohen and A. Prince, *Nat. Med.*, 2012, **18**, 509–519.
- 6 J. L. Billings, J. M. Dunitz, S. McAllister, T. Herzog, A. Bobr and A. Khoruts, *J. Clin. Gastroenterol.*, 2014, **48**, e85–e88.
- 7 C. Castellani and B. M. Assael, *Cell. Mol. Life Sci.*, 2017, **74**, 129–140.

- 8 A. T. Hastie, S. T. Hingley, F. Kueppers, M. L. Higgins, C. S. Tannenbaum and G. Weinbaum, *Infect. Immun.*, 1983, **40**, 506–513.
- 9 S. D. Carson and B. H. Bowman, *Pediatr. Res.*, 1982, **16**, 13–20.
- 10 S. C. Bell, M. A. Mall, H. Gutierrez, M. Macek, S. Madge, J. C. Davies, P. R. Burgel, E. Tullis, C. Castaños, C. Castellani, C. A. Byrnes, F. Cathcart, S. H. Chotirmall, R. Cosgriff, I. Eichler, I. Fajac, C. H. Goss, P. Drevinek, P. M. Farrell, A. M. Gravelle, T. Havermans, N. Mayer-Hamblett, N. Kashirskaya, E. Kerem, J. L. Mathew, E. F. McKone, L. Naehrlich, S. Z. Nasr, G. R. Oates, C. O'Neill, U. Pypops, K. S. Raraigh, S. M. Rowe, K. W. Southern, S. Sivam, A. L. Stephenson, M. Zampoli and F. Ratjen, *Lancet Respir. Med.*, 2020, **8**, 65–124.
- 11 V. F. Curto, C. Fay, S. Coyle, R. Byrne, C. O'Toole, C. Barry, S. Hughes, N. Moyna, D. Diamond and F. Benito-Lopez, *Sens. Actuators, B*, 2012, **171–172**, 1327–1334.
- 12 H. Y. Y. Nyein, W. Gao, Z. Shahpar, S. Emaminejad, S. Challa, K. Chen, H. M. Fahad, L. C. Tai, H. Ota, R. W. Davis and A. Javey, *ACS Nano*, 2016, **10**, 7216–7224.
- 13 L. Wang, L. Wang, Y. Zhang, J. Pan, S. Li, X. Sun, B. Zhang and H. Peng, *Adv. Funct. Mater.*, 2018, **28**, 1804456.
- 14 M. Bariya, Z. Shahpar, H. Park, J. Sun, Y. Jung, W. Gao, H. Y. Y. Nyein, T. S. Liaw, L. C. Tai, Q. P. Ngo, M. Chao, Y. Zhao, M. Hettick, G. Cho and A. Javey, *ACS Nano*, 2018, **12**, 6978–6987.
- 15 G. L. Goh, S. Agarwala, Y. J. Tan and W. Y. Yeong, *Sens. Actuators, B*, 2018, **260**, 227–235.
- 16 J. Park, D. I. Cha, Y. Jeong, H. Park, J. Lee, T. W. Kang, H. K. Lim and I. Park, *Adv. Sci.*, 2021, **8**, 2100725.
- 17 P. Nasehi, M. S. Moghaddam, N. Rezaei-Savadkouhi, M. Alizadeh, M. N. Yazdani and H. Agheli, *J. Food Meas. Charact.*, 2022, **16**, 2440–2445.
- 18 J. Liu, H. Ji, X. Lv, C. Zeng, H. Li, F. Li, B. Qu, F. Cui and Q. Zhou, *Microchim. Acta*, 2022, **189**, 54–67.
- 19 S. Nakata, M. Shiomi, Y. Fujita, T. Arie, S. Akita and K. Takei, *Nat. Electron.*, 2018, **1**, 596–603.
- 20 J. Cui, Y. Li, D. Chen, T. G. Zhan and K. Da Zhang, *Adv. Funct. Mater.*, 2020, **30**, 2005522.
- 21 X. T. Liu, X. Y. Mu, X. L. Wu, L. X. Meng, W. B. Guan, Y. Q. Ma, H. Sun, C. J. Wang and X. F. Li, *Biomed. Environ. Sci.*, 2014, **27**, 676–683.
- 22 H. J. Choi, B. C. Kang and T. J. Ha, *Biosens. Bioelectron.*, 2021, **184**, 113231.
- 23 N. Promphet, P. Rattanawaleedirojn, K. Siralermukul, N. Soatthiyanon, P. Potiyaraj, C. Thanawattano, J. P. Hinestroza and N. Rodthongkum, *Talanta*, 2019, **192**, 424–430.
- 24 Z. Stanić, Curcumin, a Compound from Natural Sources, *Plant Foods Hum. Nutr.*, 2017, **72**, 1–12.
- 25 Y. S. Musso, P. R. Salgado and A. N. Mauri, *Food Hydrocolloids*, 2017, **66**, 8–15.
- 26 B. Kuswandi, T. S. Jayus, T. S. Larasati, A. Abdullah and L. Y. Heng, *Food Anal. Methods*, 2012, **5**, 881–889.
- 27 N. Pan, J. Qin, P. Feng, Z. Li and B. Song, *J. Mater. Chem. B*, 2019, **7**, 2626–2633.
- 28 M. R. Mohammadi, S. Rabbani, S. H. Bahrami, M. T. Joghataei and F. Moayer, *Mater. Sci. Eng., C*, 2016, **69**, 1183–1191.
- 29 Z. Marković, M. Kováčová, M. Mičušík, M. Danko, H. Švajdlénková, A. Kleinová, P. Humpolíček, M. Lehotský, B. T. Marković and Z. Špitalský, *J. Appl. Polym. Sci.*, 2019, **136**, 47283.
- 30 Y. M. Tsai, W. C. Jan, C. F. Chien, W. C. Lee, L. C. Lin and T. H. Tsai, *Food Chem.*, 2011, **127**, 918–925.
- 31 X. Zhai, X. Wang, J. Zhang, Z. Yang, Y. Sun, Z. Li, X. Huang, M. Holmes, Y. Gong and M. Povey, *Food Packag. Shelf Life*, 2020, **26**, 100595.
- 32 K. Zhao, Z. H. Lu, P. Zhao, S. X. Kang, Y. Y. Yang and D. G. Yu, *Chem. Eng. J.*, 2021, **425**, 131455.
- 33 S. Shi, Y. Si, Y. Han, T. Wu, M. I. Iqbal, B. Fei, R. K. Y. Li, J. Hu and J. Qu, *Adv. Mater.*, 2022, **34**, 2107938.
- 34 S. Karagoz, N. B. Kiremitler, G. Sarp, S. Pekdemir, S. Salem, A. G. Goksu, M. S. Onses, I. Sozdutmaz, E. Sahmetlioglu, E. S. Ozkara, A. Ceylan and E. Yilmaz, *ACS Appl. Mater. Interfaces*, 2021, **13**, 5678–5690.
- 35 M. Tebyetekerwa, Z. Xu, S. Yang and S. Ramakrishna, *Adv. Fiber Mater.*, 2020, **2**, 161–166.
- 36 I. Mrsic, T. Bäuerle, S. Ulitzsch, G. Lorenz, K. Rebner, A. Kandelbauer and T. Chassé, *Appl. Surf. Sci.*, 2021, **536**, 147782.
- 37 D. Akbik, M. Ghadiri, W. Chrzanowski and R. Rohanizadeh, *Life Sci.*, 2014, **116**, 1–7.
- 38 W.-H. Lee, C.-Y. Loo, M. Bebawy, F. Luk, R. S. Mason and R. Rohanizadeh, *Curr. Neuropharmacol.*, 2013, **11**, 338–378.
- 39 J. H. Ha, J. Y. Kim, D. Kim, J. Ahn, Y. Jeong, J. Ko, S. Hwang, S. Jeon, Y. Jung, J. Gu, H. Han, J. Choi, G. Lee, M. Bok, S. A. Park, Y. S. Cho, J. H. Jeong and I. Park, *Adv. Mater. Technol.*, 2023, **8**, 2201765.